Gas hydrate decomposition recorded by authigenic barite at pockmark sites of the northern Congo Fan

Sabine Kasten · Kerstin Nöthen · Christian Hensen · Volkhard Spieß · Martin Blumenberg · Ralph R. Schneider

Abstract The geochemical cycling of barium was investigated in sediments of pockmarks of the northern Congo Fan, characterized by surface and subsurface gas hydrates, chemosynthetic fauna, and authigenic carbonates. Two gravity cores retrieved from the so-called Hydrate Hole and Worm Hole pockmarks were examined using high-resolution pore-water and solid-phase analyses. The results indicate that, although gas hydrates in the study area are stable with respect to pressure and temperature, they are and have been subject to dissolution due to methane-undersaturated pore waters. The process significantly driving dissolution is the anaerobic oxidation of methane (AOM) above the shallowest hydrate-bearing sediment layer. It is suggested that episodic seep events temporarily increase the upward flux of methane, and induce hydrate formation close to the sediment surface. AOM establishes at a sediment depth where the upward flux of methane from the uppermost hydrate layer counterbalances the downward flux of seawater sulfate. After seepage ceases, AOM continues to consume methane at the sulfate/methane transition (SMT) above the hydrates, thereby driving the progressive dissolution of the hydrates "from above". As a result the SMT migrates downward, leaving behind enrichments of authigenic barite and carbonates that typically precipitate at this biogeochemical reaction front. Calculation of the time needed to produce the observed solid-phase barium enrichments above the present-day depths of the SMT served to track the net downward migration of the SMT and to estimate the total time of hydrate dissolution in the recovered sediments. Methane fluxes were higher, and the SMT was located closer to the sediment surface in the past at both sites. Active seepage and hydrate formation are inferred to have occurred only a few thousands of years ago at the Hydrate Hole site. By contrast, AOM-driven hydrate dissolution as a consequence of an overall net decrease in upward methane flux seems to have persisted for a considerably longer time at the Worm Hole site, amounting to a few tens of thousands of years.

S. Kasten (✉) · K. Nöthen
Alfred Wegener Institute for Polar and Marine Research,
Am Handelshafen 12,
27570 Bremerhaven, Germany
e-mail: Sabine.Kasten@awi.de

C. Hensen
GEOMAR Helmholtz Centre for Ocean Research Kiel,
Wischhofstr. 1-3,
24148 Kiel, Germany

V. Spieß
University of Bremen, Department of Geosciences,
Klagenfurter Strasse,
28359 Bremen, Germany

M. Blumenberg
University of Göttingen, Geoscience Center,
Goldschmidtstr. 3,
37077 Göttingen, Germany

R. R. Schneider
Kiel University, Institute for Geosciences,
Ludewig-Meyn-Str. 10,
24118 Kiel, Germany

Introduction

Continental margin sediments host enormous amounts of methane in the form of dissolved and free gas, as well as solid gas hydrates. While numerous studies using different approaches have attempted to estimate the mass of the submarine gas hydrate reservoir (e.g., Kvenvolden 1993; Dickens 2001a; Archer et al. 2009), we still do not know the precise volume of methane stored within present-day gas

hydrate systems (for a recent review, see Dickens 2011). Moreover, gas hydrates are dynamic systems controlled by the input and output of carbon, but the magnitude of these fluxes and their evolution over time are also poorly understood and constrained (Dickens 2003, 2011).

Gas hydrates can form within a stability zone (gas hydrate stability zone, GHSZ) defined by pressure, temperature, and salinity whenever dissolved methane concentrations exceed conditions of gas hydrate saturation. The actual amount of hydrate that forms thus depends on the flux of methane into and the formation of methane within the GHSZ. The mass and distribution of hydrates can change over time when variations in pressure, temperature, and salinity (PTS), as well as in the methane saturation state of the surrounding fluids and in methane fluxes occur. The decomposition of gas hydrates induced by changes in PTS is referred to as dissociation (e.g., Brewer et al. 2002); the decomposition of gas hydrates due to methane undersaturation is termed dissolution (e.g., Egorov et al. 1999; Rehder et al. 2004; Bigalke et al. 2009; Lapham et al. 2010). Methane undersaturation in marine sediments can be produced through the sulfate-dependent anaerobic oxidation of methane (AOM; Lapham et al. 2010), which was shown to typically occur above and within gas hydrate-bearing sediments (e.g., Borowski et al. 1996, 1999; Bohrmann et al. 1998; Boetius et al. 2000; Dickens 2001b; Treude et al. 2003; Orcutt et al. 2004; Snyder et al. 2007a, b).

AOM is thought to be mediated by a consortium of methane-oxidizing archaea and sulfate-reducing bacteria (e.g., Hoehler et al. 1994; Boetius et al. 2000). It commonly occurs in a distinct sediment horizon, the sulfate/methane transition (SMT), where both sulfate and methane are consumed to depletion (e.g., Reeburgh 1976; Iversen and Jørgensen 1985; Niewöhner et al. 1998). The depth of the SMT is controlled primarily by the upward flux of methane (Borowski et al. 1999). AOM typically induces the formation of a suite of authigenic minerals including carbonates (high Mg-calcite, aragonite, and dolomite; e.g., Bohrmann et al. 1998; Aloisi et al. 2000; Greinert et al. 2001; Peckmann et al. 2001; Peckmann and Thiel 2004; Nähr et al. 2009; Meister et al. 2011) and barite (e.g., Torres et al. 1996a; Castellini et al. 2006; Riedinger et al. 2006; Snyder et al. 2007a, b). When methane reacts with sulfate at the SMT, carbonate alkalinity is increased and this leads to oversaturation with respect to carbonate minerals (e.g., Ritger et al. 1987). Diagenetic cycling of barium (Ba) occurs when barite particles—mostly biogenic barites formed in the water column in association with the degradation of organic matter—are buried below the SMT. In the sulfate-depleted sediments below the SMT, barite is undersaturated, dissolves, and Ba^{2+} is released into the pore water. Barium ions then diffuse upward into the sulfate zone, and re-precipitate as authigenic/diagenetic barite slightly above

the SMT in so-called barite fronts (e.g., Torres et al. 1996a; Dickens 2001b; Riedinger et al. 2006). The size of these diagenetic barite peaks is dependent on the upward flux of Ba^{2+} and the period of time the SMT is fixed at a particular sediment level (e.g., Dickens 2001b; Riedinger et al. 2006; Snyder et al. 2007a).

As it is essentially impossible to directly measure temporal variations in sediment methane fluxes and in the depth of the SMT, authigenic minerals that form in association with AOM—calcite and barite—have been proposed as valuable tracers (Dickens 2001b, 2003). Barite has already been successfully applied as a proxy parameter to constrain changes in the upward flux of methane from the gas hydrate system on Blake Ridge (Dickens 2001b; Snyder et al. 2007a), and from Cretaceous black shales in deposits of the Demerara Rise (Arndt et al. 2009). Recently, Nöthen and Kasten (2011) used pore-water and solid-phase Sr/Ca and Mg/Ca ratios to infer the mineralogy of authigenic carbonates in the sediments of the so-called Kouilou pockmarks of the northern Congo Fan (Sahling et al. 2008). They were able to identify active and fossil horizons of carbonate precipitation, and to reconstruct relative changes in seep activity. In addition, interstitial and solid-phase Ba data served to estimate the length of time the SMT has remained fixed at the present-day depth of the diagenetic barite fronts.

The present study expands on that of Nöthen and Kasten (2011), using the depth distribution of solid-phase Ba with the objective to track the net downward movement of the SMT, thereby giving a time perspective to changes in upward methane flux and in gas hydrate dynamics. For this purpose, gravity cores were collected from the so-called Hydrate Hole and Worm Hole pockmarks of the Kouilou pockmark field. Pore-water and solid-phase data combined with diffusive flux calculations served to estimate the time needed to precipitate the observed authigenic barium pools at each site.

Geological setting

The northern Congo Fan is located on the passive western African continental margin. It forms part of the "Aptian Salt Basins" extending from the Cameroon volcanic line in the north, to the Walvis Ridge in the south (Clifford 1986), characterized by evaporites up to 1,000 m thick (Emery and Uchupi 1984). During the middle Cretaceous (Aptian-Turonian), black shales and bituminous sandstones were deposited on top of the evaporites, the precursor of the high hydrocarbon potential of this region. Detailed descriptions of the regional sedimentological evolution and the main tectonic features are given in Gay et al. (2006a) and Savoye et al. (2009). Intensive salt diapirism and raft tectonics characterize the continental margin (e.g., Brice et al.

1982), associated with an upward migration of hydrocarbons and fluids.

Today, sedimentation on the northern Congo Fan comprises suspended material originating from the Congo River, as well as high organic matter input resulting from a mixture of high, river-induced marine productivity (Schneider et al. 1997) and terrestrial matter of various sources (Holtvoeth et al. 2001, 2003). Sedimentation rates determined by Schneider et al. (1997) for deposits of the Congo Fan vary between 3 and 17 cm 1,000 years^{-1} for the last 200,000 years. For the hemipelagic sediments of the northern Congo Fan at ODP site 1075, sedimentation rates determined by Wefer et al. (1998) are typically in the order of 10 cm 1,000 years^{-1}.

Seismic and geological data collected during several research cruises to the Congo Fan have been presented by Uenzelmann-Neben et al. (1997), Uenzelmann-Neben (1998), Ondréas et al. (2005), Gay et al. (2007), and Sahling et al. (2008). During ODP Leg 175, three holes were drilled north of the Congo Canyon (Wefer et al. 1998). The associated geophysical data revealed prominent features of focused upward fluid migration such as pockmark-like seafloor depressions and underlying columnar zones of seismic amplitude blanking. Furthermore, strong subsurface reflectors associated with these pockmark structures were interpreted as most likely representing layers enriched in gas hydrate or authigenic minerals. Recently, Andresen and Huuse (2011) reported bottom simulating reflectors associated with free gas overlain by gas hydrates in the Congo Fan.

Numerous investigations of pockmarks on the lower Congo Fan (e.g., Charlou et al. 2004; Ondréas et al. 2005; Gay et al. 2006a,b, 2007; Pierre and Fouquet 2007; Sahling et al. 2008; Haas et al. 2010; Nöthen and Kasten 2011) have revealed their association with morphologically, stratigraphically, or tectonically controlled focused fluid flow. Chemosynthetic communities, authigenic carbonates, and gas hydrates have been described for the giant Regab pockmark (see Fig. 1), which is 800 m in diameter and located close to the Congo Canyon (e.g., Charlou et al. 2004; Ondréas et al. 2005; Gay et al. 2006c), and for the Kouilou pockmarks located north of the Congo Canyon (Sahling et al. 2008; Haas et al. 2010; Nöthen and Kasten 2011).

Materials and methods

Sampling sites

Pore-water and solid-phase analyses were carried out on two gravity cores retrieved from the Hydrate Hole (GeoB 6520, 04°48.6S, 09°54.5E) and Worm Hole (GeoB 6521, 04°45.7S, 09°56.3E) pockmarks at an overall water depth of 3,100 m (Fig. 1) and a bottom water temperature of 3°C. Thus, the sites lie within the gas hydrate stability field. These are among several prominent pockmark structures identified and mapped by echosounder and seismic surveys on the northern Congo Fan during RV *Meteor* cruise M47/3 in June/July 2000 (Spieß and cruise participants 2002; Fig. 1).
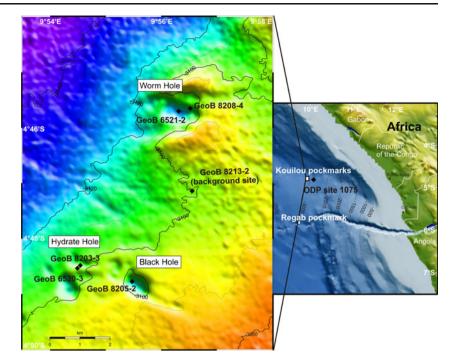
Pore-water and solid-phase sampling and analyses

After retrieval, the gravity cores were cut into 1-m segments on deck and 5-ml syringe samples were taken from every cut segment surface for methane analysis. The cores were then transported into the cold room (~4°C) of the ship where pore water was extracted by pressure filtration under an argon atmosphere, using 0.2-μm cellulose acetate membrane filters.

Samples for sulfate determination were diluted 1:20, stored frozen at −20°C, and analyzed by ion chromatography (HPLC) in the shore-based laboratory at Bremen University. For CH_4 analyses, syringe samples of wet sediment (cf. above) were filled into 50-ml septum vials containing 20 ml of a NaCl (1.2 M)/$HgCl_2$ (0.3 M) solution (Niewöhner et al. 1998). These were stored cooled (4°C) upside down until analyzed in the home laboratory where, in each case, 20 μl headspace gas was injected into a VARIAN 3400 gas chromatograph equipped with a flame ionization detector. Pore-water Ba^{2+} concentrations were determined by inductively coupled plasma optical emission spectrometry (ICP-OES) after 1:10 dilution of pore-water aliquots with 1 M HNO_3. Sediment porosity was calculated from measurements of electrical conductivity performed at 2-cm intervals (cf. Niewöhner et al. 1998; Nöthen and Kasten 2011).

Total solid-phase Ba was determined as described by Nöthen and Kasten (2011). In brief, sediment samples were taken continuously over 2-cm intervals for the Hydrate Hole core; for the Worm Hole core, samples were taken every 5 cm with cutoff syringes. After freeze drying and grinding in an agate mortar, in each case about 50 mg bulk dry sediment was digested with a mixture of ultrapure nitric (3 ml), hydrochloric (2 ml) and hydrofluoric acid (2 ml), using the microwave systems MLS Ethos 1600 and MLS Mega II at ~200°C and ~30 bar. The digested solutions were fumed off to dryness and the material re-dissolved in concentrated nitric acid (0.5 ml) and deionized water (4.5 ml), homogenized in the microwave system, filled to 50 ml with deionized water, and the major elements—including Ba—then analyzed by ICP-OES at a precision better than 3 %. Accuracy was verified using the SDO-8 standard reference material (produced in 1990 by the State University of Irkutsk and certified by the Asso Company).

Fig. 1 *Right* Bathymetric map of the Congo Fan region (modified after Sahling et al. 2008), with locations of the ODP Leg drill site 1075 (Wefer et al. 1998) and the Regab pockmark. *Left* Detailed map of the Kouilou pockmark study area (modified after Haas et al. 2010), with sampling locations at the Hydrate Hole (core GeoB 6520–2) and the Worm Hole pockmarks (core GeoB 6521–2), as well as the sites studied by Nöthen and Kasten (2011)

Calculation of barite precipitation time

To estimate the time needed to produce the observed solid-phase Ba enrichments in the Hydrate Hole and Worm Hole cores, the upward diffusive flux of Ba^{2+} into the sulfate-bearing zone above the SMT was determined based on the measured Ba^{2+} concentration gradients in pore water according to the approach applied by Dickens (2001b), Snyder et al. (2007a), and Nöthen and Kasten (2011). The diffusive flux was calculated using Fick's first law of diffusion:

$$J_{Ba}^{2+} = -\phi \times D_{sed} \times dC/dx$$

where J_{Ba}^{2+} is the diffusive flux of Ba^{2+}, ϕ the porosity, D_{sed} the tortuosity- and temperature-corrected diffusion coefficient of Ba^{2+} in the sediment, calculated from the diffusion coefficient in free solution (D_0) of 147.6 cm^2 $year^{-1}$ (5°C) after Boudreau (1997), and dC/dx is the concentration gradient of Ba^{2+} in pore water. As it is not possible to determine past changes in the upward Ba^{2+} gradient, the present-day Ba^{2+} gradients recorded at the two sites were used. Calculations are for Ba solid-phase contents exceeding 0.2 g kg^{-1}, because this value has been shown to represent the terrigenous Ba fraction in the study area (Nöthen and Kasten 2011). As even slight changes in porosity have substantial influence on the calculated enrichment times, a porosity range of 70–85 % was selected, with a grain density of 2.2 g cm^{-3}.

Results

Pockmark and core description

The two pockmarks are several hundred meters in diameter, have central depressions up to 20 m deep, and are characterized by acoustically blanked zones below (Fig. 2). Strong reflectors partly outcropping at the sediment surface likely represent hydrates, carbonate-bearing layers, or both.

The core retrieved at Hydrate Hole consists of hemipelagic sediments with only minor amounts of small authigenic carbonate precipitates, mostly close to the sediment surface. The upper 3.8 m of the core were not affected by degassing and expansion. Massive pieces of gas hydrate were found below 5 m sediment depth (Fig. 3a).
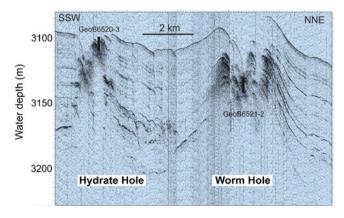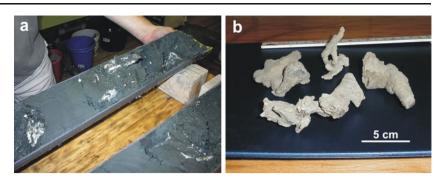

Fig. 2 Digital Parasound sediment echosounder profile running NNE–SSW across both coring sites (for more information, see main text). The vertical bars at the coring sites indicate core length; position is approximate with respect to the echosounder profile

Fig. 3 Photographs of **a** massive gas hydrates found below 5 m sediment depth in the Hydrate Hole core, and **b** large authigenic carbonate precipitates typical of the Worm Hole core

The Worm Hole core has a length of 11.5 m, and is characterized by hemipelagic sediments with numerous layers of massive carbonate precipitates (Fig. 3b). The most abundant type/morphology of authigenic carbonates were rounded irregular precipitates of up to a few centimeters in size. Gas hydrates were not recovered at this site.

The sediments recovered from the Hydrate Hole and Worm Hole would have an age of approx. 38,000 and 115,000 years, respectively, based on the average sedimentation rate of 10 cm 1,000 years^{-1} determined by Wefer et al. (1998; cf. above).

Pore water

At the Hydrate Hole site, interstitial sulfate concentrations decrease downward from seawater values in the upper part of the core into an SMT at about 2 m sediment depth (Fig. 4a). A counter-directed (upward) decline in methane concentrations into the SMT occurs from below 5 m, where massive pieces of hydrate were found. At the SMT, sulfate is not completely depleted but concentrations display a tailing and remain at about 2 mmol l^{-1} down to 3.8 m; this could result from partial oxidation of sulfide during storage. Similar to the concentration profile of methane, Ba^{2+} concentrations display an upward decrease from 35 μmol l^{-1} at 3.8 m to reach complete consumption at about 1 m (Fig. 4b).

The sulfate pore-water profile at the Worm Hole site shows a kink-type shape with a slight linear decrease in concentrations within the upper 10.5 m, and a steep decrease into the SMT located at about 11 m (Fig. 4c). Methane was not detected in this core. Interstitial Ba^{2+} concentrations are higher than at the Hydrate Hole site, and display an upward decrease from about 100 μmol l^{-1} at the base of the core to complete depletion slightly above the SMT (Fig. 4d).

Solid phase

The total solid-phase Ba contents in the upper 2.5 m of the Hydrate Hole core are overall relatively low, fluctuating at about 0.2 g kg^{-1} (Fig. 4b). At 0.2, 0.6, and 1.0 m depth, slightly elevated values reaching 0.75 g kg^{-1} are found. A
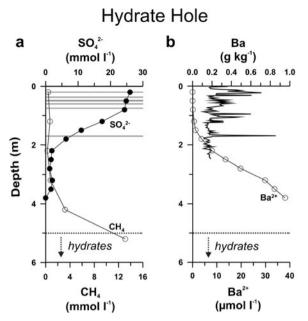
maximum Ba content of 0.85 g kg^{-1} defines a sharp peak at 1.7 m, slightly above the SMT.

At the Worm Hole site, where large authigenic carbonate precipitates occur arranged in layers throughout the core (cf. above), solid-phase Ba contents are overall substantially higher than at the Hydrate Hole site (Fig. 4d). Several pronounced Ba peaks occur above the present-day level of the SMT, with a maximum Ba content of 20 g kg^{-1} at 7.2 m depth. Baseline Ba contents are similar to the Hydrate Hole core, fluctuating at about 0.2 g kg^{-1}.

Discussion

The low baseline Ba level of 0.2 g kg^{-1} found in both investigated pockmark cores corresponds to the terrigenous Ba contents determined for the study area, contrasting with substantially higher Ba contents of about 0.8 g kg^{-1} recorded at a nearby background site not influenced by fluid seepage (core GeoB 8213–2, cf. Fig. 1; Nöthen and Kasten 2011). This finding suggests that the SMT was located closer to the sediment surface in the past at both the Hydrate Hole and the Worm Hole sites, leading to a dissolution and mobilization of the marine/biogenic Ba fraction. This is consistent with observations by Nöthen and Kasten (2011) for other seepage-influenced cores in the vicinity (cf. Fig. 1). The two cores retrieved from the Hydrate Hole and the Worm Hole investigated in the present study do, however, differ markedly from each other with respect to the presence/absence of gas hydrates, size of authigenic carbonate nodules, and magnitude of solid-phase Ba enrichments.

The Hydrate Hole pockmark core (Figs. 1 and 2) contained massive, irregularly distributed gas hydrates below 5 m sediment depth (Fig. 3a), associated with an upward-directed flux of methane into the overlying SMT at about 2.0 m (Fig. 4a), where methane is oxidized anaerobically by sulfate. The present-day depth of active authigenic barite formation slightly above the SMT at about 1.5 m is evidenced by minima in pore-water Ba^{2+} (Fig. 4b). The sharp Ba solid-phase peak of 0.85 g kg^{-1} likely represents the active diagenetic barite front (e.g., Torres et al. 1996a).
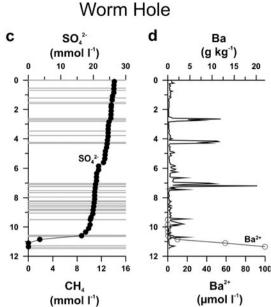
Fig. 4 a Sulfate and methane pore-water profiles, Hydrate Hole core. **b** Barium pore-water concentrations (*open circles*) and solid-phase contents (*solid line*), Hydrate Hole core. **c** Sulfate pore-water profile, Worm Hole core. **d** Barium pore-water concentrations (*open circles*) and solid-phase contents (*solid line*), Worm Hole core. Present-day SMT position: ~2 m for the Hydrate Hole site, and ~11 m for the Worm Hole site; *grey horizontal bars mark* depths where carbonate precipitates were found

The Worm Hole pockmark core contained numerous, large authigenic carbonate nodules (Fig. 3b), and the peak solid-phase Ba contents are up to 100-fold higher than at the Hydrate Hole site. Besides the actively forming diagenetic barite peak at 10.8 m indicated by a Ba content of 4.7 g kg^{-1}, the Worm Hole core has several pronounced Ba peaks above the present-day depth of the SMT (Fig. 4d). Maximum solid-phase Ba contents of up to 20 g kg^{-1} are substantially higher than those determined at other pockmark sites in the vicinity (Nöthen and Kasten 2011), and close to authigenic Ba contents reported for active mud volcanoes in the Gulf of Mexico (Castellini et al. 2006).

The authigenic carbonate precipitates as well as the solid-phase Ba peaks observed above the present-day SMT depths at the two study sites are further evidence that this biogeochemical reaction front was situated closer to the sediment surface in the past. Indeed, Dickens (2001b) argued that any decrease in the upward flux of methane should be evidenced by authigenic barite fronts located above the active depth of the diagenetic barite front. At the Hydrate Hole site, the small authigenic carbonate precipitates and Ba enrichments found (Fig. 4a, b) imply that the SMT was located about 1.8 m higher up in the past. It is possible that the observed Ba peaks could at least partly represent residues of biogenic barite remaining after partial dissolution in sulfate-depleted sediments. However, the observed concomitant occurrence of authigenic carbonates and Ba peaks suggests that they rather represent diagenetic barite.

At the Worm Hole site, the depth distribution of the massive authigenic carbonates as well as the large Ba peaks suggests that the SMT migrated downward by more than 8 m with time, leaving behind enrichments of authigenic barite and carbonates. As pointed out by Snyder et al. (2007a), the depth location of the SMT at seep sites is determined primarily by the uppermost gas hydrate layer formed by intense upward methane flux. It is likely that, after shallow gas hydrates have formed and the SMT is shifted toward the sediment surface, in situ biogenic methane formation occurs in the sulfate-depleted sediments below the SMT. However, it is here suggested that this source of methane is negligible in controlling the depth position of the SMT compared to the amount of methane supplied from deeper sources during a seep event, and temporarily trapped and concentrated in the form of gas hydrate. Furthermore, organic matter depositing on the Congo Fan is strongly enriched in terrigenous material (Schneider et al. 1997; Holtvoeth et al. 2001, 2003), implying that the overall reactivity of the bulk organic matter for methane formation is comparatively low. It is therefore argued that the SMT at the Worm Hole site has experienced a *net* downward migration of more than 8 m since the most intense past fluid migration and hydrate-forming event, which shifted the SMT close to the (former) sediment surface. It is indeed possible that the SMT did not migrate downward continuously but rather fluctuated over the examined sediment interval, considering the episodic nature of seepage at pockmark sites and the repeated pulses of upward methane flux

that are likely to have occurred (e.g., Hovland and Judd 1988; Gay et al. 2007).

The process likely to have caused the observed net downward progression of the SMT after periods of higher upward methane flux is the undersaturation of methane in the sediments overlying the gas hydrates, as already pointed out by Dickens (2001a, 2003). The dissolution of gas hydrates driven by methane undersaturation of the surrounding bottom waters or pore waters has been the subject of several studies (e.g., Egorov et al. 1999; Dickens 2001a, 2003; Rehder et al. 2004; Bigalke et al. 2009). Only recently, Lapham et al. (2010) presented the first high-resolution in situ methane pore-water profiles of sediments overlying deep-sea gas hydrates of the northern Cascadia margin and the northern Gulf of Mexico. Their measurements revealed that the pore fluids of sediments immediately surrounding the gas hydrate deposits were largely undersaturated with respect to methane concentration in equilibrium with methane gas hydrate, and that AOM accounted for some of this undersaturation.

The sulfate and methane pore-water profiles at the Hydrate Hole site (Fig. 4a) demonstrate that AOM occurs roughly 3 m above the hydrate-bearing sediments. The consumption of methane at the SMT establishes a concentration gradient between the uppermost hydrate layer and the SMT that is steeper than the gradient that would exist between the hydrate layer and the bottom water in the absence of AOM. Although this is a theoretical consideration—because AOM always occurs above sediment-covered marine gas hydrates—it demonstrates that AOM steepens the upward methane gradient, increases the upward methane flux from the top of the hydrates, and thereby drives or at least accelerates hydrate dissolution. Thus, the upward diffusive escape of methane drives the progressive dissolution of the gas hydrates from above as long as no re-charge of the gas hydrates by a new fluid migration event occurs and nourishes carbonate formation in the overlying SMT. Based on these considerations it is here proposed that, although gas hydrates were not found in the Worm Hole core, they were indeed present at shallow sediment depths at the Worm Hole site in the past. In fact, the formation of the observed massive carbonate nodules and the fixation of the SMT at a particular horizon for a period long enough to produce the observed strong solid-phase Ba enrichments would not have been possible in the absence of gas hydrates in those earlier times.

A downward SMT shift accompanied by diagenetic barite precipitation has also been suggested by Arndt et al. (2009) for deposits of the Demerara Rise (equatorial Atlantic, ODP Leg 207). Authigenic barite enrichments spanning over several tens to hundreds of meters sediment depth were interpreted as indicating a more or less continuous downward shift of the SMT with time, driven by decreasing rates of methanogenesis within deeply buried black shale layers. Although their system differs significantly from the pockmark sites of the present study, this highlights the potential of Ba to trace the downward migration of the SMT and changes in the rates of formation and upward fluxes of hydrocarbons. In contrast to the Demerara Rise study site, the distinct peaks and extremely high concentrations of Ba found in the Worm Hole core mark depths where the SMT would have been fixed for a considerable length of time. Such a non-continuous downward progression of the SMT is in accordance with the typically irregular distribution of hydrates in layers and veins of Kouilou pockmarks examined to date (Spieß and cruise participants 2002; Sahling et al. 2008). It is suggested that, after the uppermost hydrate layer has dissolved (driven/accelerated by AOM), the SMT will move down and reestablish at greater sediment depth above the next gas hydrate-bearing sediment horizon, consistent with the conceptual model of Dickens (2001b). The magnitude of authigenic carbonate enrichment and barite formation would be a function of the upward flux of Ba^{2+}, and the amount of time the SMT persisted at a particular depth above the uppermost hydrate-bearing sediment layer.

For sediments overlying gas hydrates of the deep-sea Niger Delta, a sub-Recent downward movement of the zone of AOM has also been suggested by Henderson et al. (2006). Based on U/Th dating of authigenic carbonates and modeling of pore-water data, those authors proposed that SMT migration was induced by responses of that deep-water gas hydrate reservoir to environmental changes related to late Quaternary climate, presumably dissociation of hydrates during the Holocene thermal maximum. However, it is here suggested that this explanation is rather unlikely because, in deep-water environments such as that of the present study, warming dissociates gas hydrate at the bottom of the GHSZ, rather than affecting gas hydrate stability at the top of the GHSZ (Dickens 2001a). Shallow gas hydrates as found on the deep Congo Fan would therefore not be impacted (cf. Sultan et al. 2004), and one can exclude that gas hydrate decomposition at the deep-water Kouilou pockmark sites is or was brought about by any changes in external conditions—and thus is not driven by dissociation.

It has been shown that, at times of vigorous upward fluid flow, Ba-rich fluids can episodically be expelled into the bottom water, inducing the formation of barite chimneys or barite precipitation onto the seafloor (e.g., Torres et al. 1996b; Aloisi et al. 2004; Castellini et al. 2006). For mud volcanoes in the northern Gulf of Mexico, Castellini et al. (2006) report evidence that smooth barite-rich carbonate nodules—such as those of the Worm Hole core—form when the SMT remains fixed for a considerable period of time. This argues against Ba-rich fluid venting and subsequent barite precipitation on the seafloor as confounding factor within the present context. The amount of diagenetic Ba that

Table 1 Calculation of precipitation time of solid-phase barium enrichments (>0.2 gkg^{-1}) in sediments of the Hydrate Hole core (GeoB 6520–3) and the Worm Hole core (GeoB 6521–2)

Station GeoB	Site	Ba gradient[a] (mol cm^{-3} cm^{-1})	Porosity (%)	Ba flux (mol cm^{-2} year^{-1})	Period of time (years)
6520-3	Hydrate Hole	1.97E-10	85	1.96E-08	1,511
			80	1.69E-08	2,337
			75	1.46E-08	3,394
			70	1.25E-08	4,745
6521-2	Worm Hole	1.80E-09	85	1.80E-07	12,904
			80	1.55E-07	19,953
			75	1.33E-07	28,978
			70	1.15E-07	40,521

[a] Assumed to be constant over time. Grain density: 2.2 g cm^{-3}

precipitated above the present-day SMT depths at the Hydrate Hole and Worm Hole sites can thus be used to calculate (1) the time the SMT remained fixed at the particular sediment depths, and (2) the total time of net downward SMT migration after the most intense fluid migration event.

Barite precipitation time

Calculations of the time needed to produce all solid-phase Ba enrichments exceeding 0.2 g kg^{-1} at and above the present-day SMT depths at the Hydrate Hole and Worm Hole sites can be used to approximate the total time of gas hydrate dissolution, and to roughly date the last most intense fluid migration event at each site. At the Hydrate Hole site, the occurrence of hydrates at shallow depth (i.e., below 5 m), and of only very small carbonate concretions and minor authigenic Ba enrichments suggests that the last fluid migration event and the formation of hydrates occurred much more recently than at the Worm Hole site.

Depending on the porosity chosen, the time span needed to form all Ba enrichments exceeding 0.2 g kg^{-1} for the Hydrate Hole core varies from 4,745 years (70 % porosity) to 1,511 years (85 % porosity; Table 1). The corresponding values for the Worm Hole core are 40,521 years (70 % porosity) to 12,904 years (85 % porosity). Although these are only very rough estimates, they suggest that gas hydrate dissolution persisted for a considerably longer period of time at the Worm Hole site. This supports the interpretation (cf. above) that the last hydrate-forming fluid migration event is likely to have occurred much more recently at the Hydrate Hole site (a few thousands of years ago) than at the Worm Hole location (a few tens of thousands of years ago).

These findings suggest that the two investigated pockmark sites are today in a less active phase of fluid seepage, and that the dissolution of the gas hydrates formed during the last fluid-venting episodes is the key driver of downward SMT migration. Indeed, other studies on the northern Congo Fan have shown that most of the pockmarks are today relatively dormant (Gay et al. 2007; Sahling et al. 2008; Nöthen and Kasten 2011). Moreover, the present findings are consistent with the general observation that fluid migration within pockmarks is highly variable both spatially and temporally, and imply that individual venting events in the study area are not triggered by changes in single external factors.

Conclusions

Although AOM-driven dissolution of gas hydrates is slow compared to the decomposition of hydrates in direct contact with low-methane seawater (e.g., Egorov et al. 1999), or to dissociation under conditions outside the hydrate stability field (e.g., Suess et al. 1999; Torres et al. 2002), estimation of the long-term existence/stability of gas hydrate reservoirs over geologic timescales is of fundamental relevance for paleoclimatic, paleoceanographic, and paleoenvironmental reconstructions. Evaluation of the size as well as the spatiotemporal dynamics of gas hydrate systems is urgently needed to incorporate these vast CH$_4$ reservoirs into models of the global carbon cycle, and the requirement for improved proxies is by now well recognized (e.g., Dickens 2003; Nöthen and Kasten 2011). The present study is the first to successfully use diagenetic barite to quantitatively track the net downward migration of the SMT resulting from gas hydrate dissolution. The findings also emphasize that, in contrast to hydrate dissociation, hydrate dissolution induced/accelerated by AOM does not automatically imply a significant release of methane-derived carbon into the water column, because the bicarbonate ions produced by methane oxidation are mostly trapped within the sediment as authigenic carbonates.

References

Aloisi G, Pierre C, Rouchy J, Foucher J, Woodside J, MEDINAUT Scientific Party (2000) Methane-related authigenic carbonates of eastern Mediterranean Sea mud volcanoes and their possible relation to gas hydrate destabilization. Earth Planet Sci Lett 184:321–338

Aloisi G, Wallmann K, Bollwerk SM, Derkachev A, Bohrmann G, Suess E (2004) The effect of dissolved barium on biogeochemical processes at cold seeps. Geochim Cosmochim Acta 68:1735–1748

Andresen KJ, Huuse M (2011) 'Bulls-eye' pockmarks and polygonal faulting in the Lower Congo Basin: relative timing and implications for fluid expulsion during shallow burial. Mar Geol 279:111–127

Archer D, Buffett B, Brovkin V (2009) Ocean methane hydrate as a slow tipping point in the global carbon cycle. Proc Natl Acad Sci 106:20596–20601

Arndt S, Hetzel A, Brumsack H-J (2009) Evolution of organic matter degradation in Cretaceous black shales inferred from authigenic barite: a reaction-transport model. Geochim Cosmochim Acta 73:2000–2022

Bigalke NK, Rehder G, Gust G (2009) Methane hydrate dissolution rates in undersaturated seawater under controlled hydrodynamic forcing. Mar Chem 115:226–234

Boetius A, Ravenschlag K, Schubert CJ, Rickert D, Widdel F, Gieseke A, Amann R, Jørgensen BB, Witte U, Pfannkuche O (2000) A marine microbial consortium apparently mediating anaerobic oxidation of methane. Nature 407:623–626

Bohrmann G, Greinert J, Suess E, Torres M (1998) Authigenic carbonates from the Cascadia subduction zone and their relation to gas hydrate stability. Geology 26:647–650

Borowski WS, Paull CK, Ussler W III (1996) Marine pore-water sulfate profiles indicate in situ methane flux from underlying gas hydrate. Geology 24:655–658

Borowski WS, Paull CK, Ussler W III (1999) Global and local variations of interstitial sulfate gradients in deep-water, continental margin sediments: sensitivity to underlying methane and gas hydrates. Mar Geol 159:131–154

Boudreau BP (1997) Diagenetic models and their implementation – Modelling transport and reactions in aquatic sediments. Springer, Berlin

Brewer PG, Paull C, Peltzer ET, Ussler W, Rehder G, Friederich G (2002) Measurements of the fate of gas hydrates during transit through the ocean water column. Geophys Res Lett 29(22):2081. doi:10.1029/2002GL014727

Brice SE, Cochran MD, Pardo G, Edwards AD (1982) Tectonics and sedimentation of the South Atlantic rift sequence: Cabinda,

Angola. In: Watkins JS, Drake CL (eds) Studies in continental margin geology. Am Assoc Petrol Geol Memoir 34:5–18

Castellini DG, Dickens GR, Snyder GT, Ruppel CD (2006) Barium cycling in shallow sediment above active mud volcanoes in the Gulf of Mexico. Chem Geol 226:1–30

Charlou JL, Donval JP, Fouquet Y, Ondréas H, Knoery J, Cochonat P, Levaché D, Poirier Y, Jean-Baptiste P, Fourré E, Chazallon B, The ZAIROV Leg 2 Scientific Party (2004) Physical and chemical characterization of gas hydrates and associated methane plumes in the Congo-Angola Basin. Chem Geol 205:405–425

Clifford AC (1986) African oil – past, present, and future. In: Halbouty MT (ed) Future petroleum provinces of the world. Am Assoc Petrol Geol Memoir 40:339–372

Dickens GR (2001a) The potential volume of oceanic methane hydrates with variable external conditions. Org Geochem 32:1179–1193

Dickens GR (2001b) Sulfate profiles and barium fronts in sediment on the Blake Ridge: present and past methane fluxes through a large gas hydrate reservoir. Geochim Cosmochim Acta 65:529–543

Dickens G (2003) Rethinking the global carbon cycle with a large, dynamic and microbially mediated gas hydrate capacitor. Earth Planet Sci Lett 213:169–183

Dickens G (2011) Down the rabbit hole: toward appropriate discussion of methane release from gas hydrate systems during the Paleocene-Eocene thermal maximum and other past hyperthermal events. Clim Past 7:831–846

Egorov AV, Crane K, Vogt PR, Rozhkov AN, Shirshov PP (1999) Gas hydrates that outcrop on the sea floor: stability models. Geo-Mar Lett 19(1/2):68–75. doi:10.1007/s003670050094

Emery KO, Uchupi E (1984) The geology of the Atlantic Ocean. Springer, New York

Gay A, Lopez M, Cochonat P, Levaché D, Sermondadaz G, Seranne M (2006a) Evidences of early to late fluid migration from an upper Miocene turbiditic channel revealed by 3D seismic coupled to geochemical sampling within seafloor pockmarks, Lower Congo Basin. Mar Petrol Geol 23:387–399

Gay A, Lopez M, Cochonat P, Seranne M, Levaché D, Sermondadaz G (2006b) Isolated seafloor pockmarks linked to BSRs, fluid chimneys, polygonal faults and stacked Oligocene-Miocene turbiditic palaeochannels in the Lower Congo Basin. Mar Geol 226:25–40

Gay A, Lopez M, Ondréas H, Charlou JL, Sermondadaz G, Cochonat P (2006c) Seafloor facies related to upward methane flux within a Giant Pockmark of the Lower Congo Basin. Mar Geol 226:81–95

Gay A, Lopez M, Berndt C, Seranne M (2007) Geological controls on focused fluid flow associated with seafloor seeps in the Lower Congo Basin. Mar Geol 244:68–92

Greinert J, Bohrmann G, Suess E (2001) Gas hydrate-associated carbonates and methane-venting at Hydrate Ridge: classification, distribution, and origin of authigenic lithologies. In: Paull CK, Dillon WP (eds) Natural gas hydrates: occurrence, distribution, and detection. Geophys Monogr 124:99–113

Haas A, Peckmann J, Elvert M, Sahling H, Bohrmann G (2010) Patterns of carbonate authigenesis at the Kouilou pockmarks on the Congo deep-sea fan. Mar Geol 268:129–136

Henderson GM, Bayon G, Pierre C, Caprais JC, Voisset M (2006) Constraints on the dynamics of gas hydrates in Niger Delta sediments from U/Th dating of cold-seep carbonates. Goldschmidt Conf Abstr A25. doi:10.1016/j.gca2006.06.494

Hoehler T, Alperin MJ, Albert DB, Martens C (1994) Field and laboratory studies of methane oxidation in an anoxic marine sediment: evidence for a methanogen-sulfate reducer consortium. Global Biogeochem Cycles 8:451–463

Holtvoeth J, Wagner T, Horsfield B, Schubert CJ, Wand U (2001) Late-Quaternary supply of terrigenous organic matter to the Congo deep-sea fan (ODP site 1075): implications for equatorial African

paleoclimate. Geo-Mar Lett 21(1):23–33. doi:10.1007/s003670100060

Holtvoeth J, Wagner T, Schubert CJ (2003) Organic matter in river-influenced continental margin sediments: the land-ocean and climate linkage at the Late Quaternary Congo fan (ODP Site 1075). Geochem Geophys Geosys 4:1109. doi:10.1029/2003GC000590

Hovland M, Judd AG (1988) Seabed pockmarks and seepage. Impact on geology, biology and the marine environment. Graham & Trotman, London

Iversen N, Jørgensen BB (1985) Anaerobic methane oxidation rates at the sulfate-methane transition in marine sediments from Kattegat and Skagerrak (Denmark). Limnol Oceanogr 30:944–955

Kvenvolden KA (1993) Gas hydrates: geological perspective and global change. Rev Geophys 31:173–187

Lapham L, Chanton JP, Chapman R, Martens CS (2010) Methane under-saturated fluids in deep-sea sediments: implications for gas hydrate stability and rates of dissolution. Earth Planet Sci Lett 298:275–285

Meister P, Gutjahr M, Frank M, Bernasconi SM, Vasconcelos C, McKenzie JA (2011) Dolomite formation within the methanogenic zone induced by tectonically driven fluids in the Peru accretionary prism. Geology 39:563–566

Nähr TH, Birgel D, Bohrmann G, MacDonald IR, Kasten S (2009) Biogeochemical controls on authigenic carbonate formation at the Chapopote "asphalt volcano", Bay of Campeche. Chem Geol 266:390–402

Niewöhner C, Hensen C, Kasten S, Zabel M, Schulz HD (1998) Deep sulfate reduction completely mediated by anaerobic methane oxidation in sediments of the upwelling area off Namibia. Geochim Cosmochim Acta 62:455–464

Nöthen K, Kasten S (2011) Reconstructing changes in seep activity by means of pore water and solid phase Sr/Ca and Mg/Ca ratios in pockmark sediments of the Northern Congo Fan. Mar Geol 287:1–13

Ondréas H, Olu K, Fouquet Y, Charlou JL, Gay A, Dennielou B, Donval JP, Fifis A, Nadalig T, Cochonat P, Cauquil E, Bourillet JF, Le Moigne M, Sibuet M (2005) ROV study of a giant pockmark on the Gabon continental margin. Geo-Mar Lett 25(5):281–292. doi:10.1007/s00367-005-0213-6

Orcutt BN, Boetius A, Lugo SK, MacDonald IR, Samarkin VA, Joye SB (2004) Life at the edge of methane ice: microbial cycling of carbon and sulfur in Gulf of Mexico gas hydrates. Chem Geol 205:239–251

Peckmann J, Thiel V (2004) Carbon cycling at ancient methane-seeps. Chem Geol 205:443–467

Peckmann J, Reimer A, Luth U, Luth C, Hansen BT, Heinicke C, Hoefs J, Reitner J (2001) Methane-derived carbonates and authigenic pyrite from the northwestern Black Sea. Mar Geol 177:129–150

Pierre C, Fouquet Y (2007) Authigenic carbonates from methane seeps of the Congo deep-sea fan. Geo-Mar Lett 27(2/4):249–257. doi:10.1007/s00367-007-0081-3

Reeburgh WS (1976) Methane consumption in Cariaco trench waters and sediments. Earth Planet Sci Lett 28:337–344

Rehder G, Kirby SH, Durham WB, Stern LA, Peltzer ET, Pinkston J, Brewer PG (2004) Dissolution rates of pure methane hydrate and carbon-dioxide hydrate in undersaturated seawater at 100-m depth. Geochim Cosmochim Acta 68:285–292

Riedinger N, Kasten S, Gröger J, Franke C, Pfeifer K (2006) Active and buried authigenic barite fronts in sediments from the Eastern Cape Basin. Earth Planet Sci Lett 241:876–887

Ritger S, Carson B, Suess E (1987) Methane-derived authigenic carbonates formed by subduction-induced pore-water expulsion along the Oregon/Washington margin. Geol Soc Am Bull 98:147–156

Sahling H, Bohrmann G, Spiess V, Bialas J, Breitzke M, Ivanov M, Kasten S, Krastel S, Schneider R (2008) Pockmarks in the Northern Congo Fan area, SW Africa: complex seafloor features shaped by fluid flow. Mar Geol 249:206–225

Savoye B, Babonneau N, Dennielou B, Bez M (2009) Geological overview of the Angola-Congo margin, the Congo deep-sea fan and its submarine valleys. Deep-Sea Res I 56:2169–2182

Schneider RR, Price B, Müller PJ, Kroon D, Alexander I (1997) Monsoon related variations in Zaire (Congo) sediment load and influence of fluvial silicate supply on marine productivity in the east equatorial Atlantic during the last 200,000 years. Paleoceanography 12:463–481

Snyder GT, Dickens GR, Castellini DG (2007a) Labile barite contents and dissolved barium concentrations on Blake Ridge: new perspectives on barium cycling above gas hydrate systems. J Geochem Explor 95:48–65

Snyder GT, Hiruta A, Matsumoto R, Dickens GR, Tomaru H, Takeuchi R, Komatsubara J, Ishida Y, Yu H (2007b) Pore water profiles and authigenic mineralization in shallow marine sediments above the methane-charged system on Umitaka Spur, Japan Sea. Deep-Sea Res II 54:1216–1239

Spieß V, cruise participants (2002) Report and preliminary results of METEOR-Cruise M 47/3, Libreville – Walvis Bay, 01.06. – 03.07.2000. Berichte Reports, Fachbereich Geowissenschaften, Universität Bremen, no 202

Suess E, Torres ME, Bohrmann G, Collier J, Greinert J, Linke P, Rehder G, Tréhu A, Wallmann K, Winckler G, Zuleger E (1999) Gas hydrate destabilization: enhanced dewatering, benthic material turnover and large methane plumes at the Cascadia margin. Earth Planet Sci Lett 170:1–15

Sultan N, Cochonat P, Foucher J-P, Mienert J (2004) Effect of gas hydrates melting on seafloor slope instability. Mar Geol 213:379–401

Torres ME, Brumsack HJ, Bohrmann G, Emeis KC (1996a) Barite fronts in continental margin sediments: a new look at barium remobilization in the zone of sulfate reduction and formation of heavy barites in diagenetic fronts. Chem Geol 127:125–139

Torres ME, Bohrmann G, Suess E (1996b) Authigenic barites and fluxes of barium associated with fluid seeps in the Peru subduction zone. Earth Planet Sci Lett 144:469–481

Torres M, McManus J, Hammond DE, de Angelis MA, Heeschen KU, Colbert SL, Tryon MD, Brown KM, Suess E (2002) Fluid and chemical fluxes in and out of sediments hosting methane hydrate deposits on Hydrate Ridge, OR, I: Hydrological provinces. Earth Planet Sci Lett 201:525–540

Treude T, Boetius A, Knittel K, Wallmann K, Jørgensen BB (2003) Anaerobic oxidation of methane above gas hydrates at Hydrate Ridge, NE Pacific Ocean. Mar Ecol Prog Ser 264:1–14

Uenzelmann-Neben G (1998) Neogene sedimentation history of the Congo Fan. Mar Petrol Geol 15:635–650

Uenzelmann-Neben G, Spieß V, Bleil U (1997) A seismic reconnaissance survey of the northern Congo Fan. Mar Geol 140:283–306

Wefer G, Berger WH, Richter C et al (1998) Proc ODP, initial reports, vol 175. Ocean Drilling Program, College Station